Wavelength-dependent optical bleaching in Al_2O_3:C nanoDot optically stimulated luminescence dosimeters

Isabel Morales-Peña and Miguel Ángel Camacho-López

Laboratorio de Fotomedicina, Biofotónica y Espectroscopia Láser de Pulsos Ultracortos, Facultad de Medicina, Universidad Autónoma del Estado de México (UAEMex), Toluca, Mexico.

Olivia Amanda García-Garduño

Laboratorio de Física Médica, Instituto Nacional de Neurología y Neurocirugía, Mexico City, Mexico.

Rosalia Contreras-Bulnes

Facultad de Odontología, Universidad Autónoma del Estado de México (UAEMex), Toluca, Mexico.

Received 7 April 2026; accepted 12 June 2026

The reusability of Al_2O_3:C-based optically stimulated luminescence dosimeters (OSLDs) relies on efficient removal of the stored signal through optical irradiation. Wavelength-dependent optical bleaching was evaluated in nanoDot^{TM} dosimeters using 3 W LED matrices centered at 463 and 516 nm, with irradiances of 587.7 and 457.7 mW·cm^{-2}, respectively. Dosimeters irradiated with 6 MV photons were subjected to successive 5-min bleaching cycles with intermediate microStar readouts. The 463 nm system produced faster signal reduction and higher bleaching efficiency than the 516 nm system. A residual component persisted after prolonged irradiation, indicating incomplete depletion of optically accessible trapping states under the evaluated conditions. These results support wavelength selection as a key parameter for optimizing nanoDot reuse protocols.

Keywords: Optically stimulated luminescence dosimeters; optical bleaching; wavelength dependence; Al_2O_3:C; residual signal; clinical dosimetry.

DOI: https://doi.org/10.31349/RevMexFis.72.061102

1. Introduction

Optically stimulated luminescence (OSL) is a widely used technique in ionizing radiation dosimetry due to its high sensitivity, stability, and capability for repeated, non-destructive readout [1]. In particular, Al_2O_3:C-based dosimeters, such as nanoDot^{TM} devices, have demonstrated robust performance in clinical applications owing to their wide dynamic range and reproducibility [2].

At the microscopic level, OSL behavior in Al_2O_3:C is associated with crystal defects induced by carbon doping, which introduce energy levels within the bandgap. Among these defects, F and F^+ centers—related to oxygen vacancies acting as electron traps—as well as recombination centers responsible for luminescent emission, play a key role [3]. Upon irradiation with ionizing radiation, charge carriers are promoted to the conduction band and subsequently trapped in metastable states. Optical stimulation releases these electrons, producing a luminescent signal proportional to the absorbed dose [4].

The removal of the stored signal, known as bleaching, is essential for OSLD reuse. However, its efficiency is strongly influenced by the energy distribution of traps in the material. In Al_2O_3:C, both shallow traps—efficiently emptied by optical irradiation—and deep traps—limiting complete signal removal—coexist [5].

The probability of optical release of trapped electrons depends on the photon energy, introducing a direct wavelength dependence in the bleaching process. Shorter wavelengths (higher photon energy) generally enhance photoionization rates, increasing bleaching efficiency, whereas longer wavelengths are less effective in depopulating certain trap populations [6].

Additionally, phototransfer phenomena have been reported, in which electrons trapped in deep levels are promoted to optically active traps, contributing to residual signal even after prolonged optical irradiation [7]. This behavior imposes limitations on bleaching efficiency and measurement reproducibility.

From a kinetic standpoint, the reduction of the OSL signal during optical irradiation can be approximated by effective exponential models, which allow characterization of trap depopulation dynamics through time constants and related parameters such as the process half-life [8]. These parameters provide useful metrics for comparing bleaching efficiency under different experimental conditions.

In this context, the present study aims to evaluate the bleaching efficiency of Al_2O_3:C nanoDot^{TM} dosimeters under optical irradiation at 463 nm and 516 nm. The analysis is based on normalized signal evolution, monoexponential fitting of decay curves, and determination of characteristic parameters such as half-life and residual signal, in order to establish a quantitative comparison between both irradiation systems. The primary objective of this work is to provide a quantitative assessment of monochromatic LED-based optical bleaching systems and their applicability to

nanoDot$^{\mathrm{TM}}$ reuse protocols under controlled experimental conditions, rather than to identify the fundamental trapping mechanisms responsible for the observed luminescence behavior.

Theoretical framework

The characterization of the optical bleaching process in optically stimulated luminescence dosimeters requires a quantitative description of signal decay under optical irradiation. From an experimental perspective, the primary objective is to compare the rate and efficiency of signal removal through measurable parameters, rather than relying solely on qualitative descriptions of signal reduction. In this context, the analysis of normalized decay curves and their fitting using exponential functions constitutes a widely adopted approach for describing the effective dynamics of electron trap depopulation [4, 8].

When the signal decay is governed by an effective population of traps, the behavior can be approximated by a monoexponential model:

$$I(t) = I_b + A\exp(-t/\tau),$$

where $I(t)$ is the measured signal after a cumulative optical irradiation time t, I_b corresponds to the baseline signal of the system, A represents the removable signal amplitude, and τ is the characteristic time constant of the process. This formulation allows bleaching to be described as an effective decay process without explicitly accounting for the individual contributions of each trap population present in the material [4, 9].

From this expression, the half-life of the process is defined as:

$$t_{1/2} = \tau \ln 2,$$

The half-life provides a direct parameter for comparison between different experimental conditions, as it represents the time required for the signal to decrease to half of its initial value. In OSL dosimetry studies, this parameter is commonly used as a practical metric to evaluate bleaching rate and compare different optical stimulation systems [8].

Since the initial OSL signal depends on the absorbed dose, normalization is required to compare results across different conditions. The ratio $I(t)/I_0$, where I_0 is the initial signal prior to bleaching, allows analysis of the remaining signal fraction independently of absolute signal magnitude. This approach is consistent with methodologies reported in the literature for analyzing decay processes in OSL dosimetry [1, 5].

However, when the residual signal approaches values close to the detection limit, the contribution of the system baseline becomes significant. For this reason, the ratio $I(t)/I_b$, where I_b represents the experimentally determined background signal, provides a useful metric to evaluate the degree of approach to the baseline state of the dosimeter. This relationship is particularly relevant for defining the practical limit of bleaching, as a residual signal approaching I_b indicates effective emptying of optically accessible traps [1, 2, 9].

The inclusion of the term I_b in the decay model also allows discrimination between actual signal removal and limitations imposed by the measurement system. In this sense, the baseline signal should not be interpreted solely as instrumental noise, but rather as an experimental reference defining the minimum observable signal level in the reader–dosimeter system [9].

Although the actual bleaching process may involve multiple trap populations and complex kinetics, the use of a monoexponential model is appropriate when the objective is to perform quantitative comparisons between experimental conditions. This type of approximation has been widely employed to describe effective decay processes in luminescent materials, enabling the extraction of reproducible parameters without overfitting the data [10, 11].

Under this framework, bleaching efficiency can be evaluated based on three primary parameters: the time constant τ, the half-life $t_{1/2}$, and the residual term associated with the baseline signal.

2. Materials and methods

2.1. Materials

Twenty Al_2O_3:C optically stimulated luminescence dosimeters (nanoDot$^{\mathrm{TM}}$, Landauer Inc.) were used in this study. All dosimeters were selected from the same batch in order to minimize sensitivity variations. The detectors were divided into two groups of ten units, assigned to optical irradiation conditions at wavelengths of 463 nm and 516 nm.

OSL signal readout was performed using a microStar reader, which provides an integrated signal corresponding to the luminescent emission during the readout cycle.

Prior to experimental use, the dosimeters were subjected to optical irradiation cycles to reduce residual signals associated with manufacturing and storage conditions, thereby establishing reproducible initial conditions. All handling and experimental procedures were conducted in accordance with the recommendations of the AAPM TG-191 report [13].

2.2. Irradiation

Irradiations were performed using a clinical linear accelerator TrueBeam STx (Varian Medical Systems, USA) delivering a 6 MV photon beam.

Beam calibration was carried out following the TRS-398 protocol established by the International Atomic Energy Agency (IAEA), using a Farmer-type ionization chamber as the reference detector [14].

The nanoDot$^{\mathrm{TM}}$ dosimeters were irradiated with absorbed doses ranging from 0.25 to 5 Gy using a 6 MV photon beam generated by a Varian TrueBeam STx linear accelerator (Varian Medical Systems, USA). Irradiations were performed

in a Solid Water phantom under reference dosimetry conditions following the IAEA TRS-398 protocol. The dosimeters were positioned at a depth of 5 cm, with 5 cm of Solid Water above and 5 cm below the detectors, at a source-to-surface distance (SSD) of 100 cm and using a 10×10 cm^2 irradiation field. These conditions ensured accurate and reproducible dose delivery throughout the study.

After irradiation, the dosimeters were stored under controlled lighting conditions to prevent unintended optical exposure prior to the bleaching process.

2.3. Optical irradiation system

For the optical bleaching process, LED-based irradiation modules were developed. Each module consisted of a 5×2 matrix arrangement of high-power LEDs mounted on a 20×15 cm acrylic base.

Two independent modules were constructed with central wavelengths of 463 nm and 516 nm, corresponding to the blue and green spectral regions, respectively. The LEDs used were commercial 3 W devices connected in series.

To ensure reproducible geometry, laser-cut acrylic positioning plates were incorporated, allowing precise placement of the dosimeters during optical irradiation.

This configuration provided an approximately uniform optical irradiance over the sensitive area of the detectors. The irradiance at the dosimeter position was estimated to be 587.7 mW·cm^{-2} for the 463 nm module and 457.7 mW·cm^{-2} for the 516 nm module.

2.4. Experimental protocol for optical bleaching

The dosimeters were initially irradiated with a 6 MV photon beam at the prescribed dose levels. Following the recommendations of AAPM TG-191, all dosimeters were allowed to stabilize for 15 min after irradiation before the initial readout. This delay was kept constant throughout the study. The signal measured after this stabilization period was defined as I_0 and used as the reference value for normalization.

Subsequently, each dosimeter was subjected to optical irradiation in successive 5-minute cycles. After each irradiation interval, the dosimeters were removed from the optical irradiation system and allowed to stabilize for 15 min before readout, following the same procedure adopted for the initial measurement. The corresponding signal I(t) was then recorded for each cumulative optical irradiation time.

This optical irradiation–readout sequence (as illustrated in Fig. 1) was repeated sequentially until a total accumulated irradiation time of 60 minutes was reached, generating a discrete dataset of OSL signal as a function of time.

2.5. OSL signal definition and curve construction

Based on the described experimental protocol, the OSL signal $I(t)$ corresponds to the integrated value provided by the reader at each measurement interval, where t represents the cumulative optical irradiation time. Each data point represents the mean value obtained from ten dosimeters.

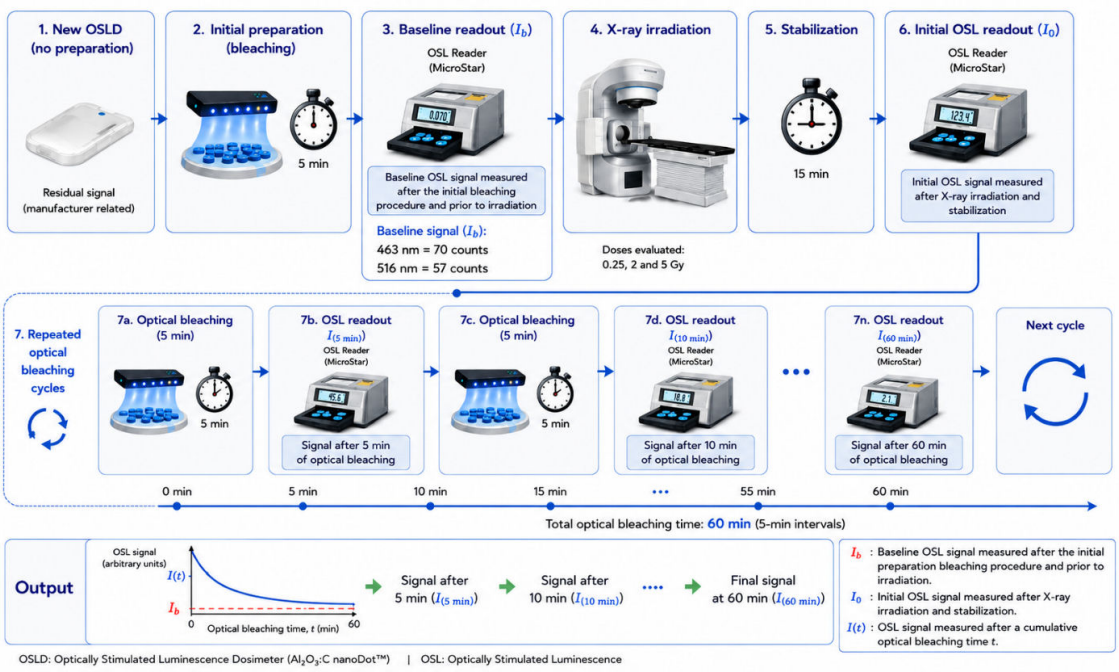


FIGURE 1. Schematic representation of the experimental protocol used for optical bleaching of Al_2O_3:C nanoDot^{TM} OSL dosimeters under 463 nm and 516 nm irradiation. I_b denotes the baseline OSL signal measured after the initial preparation bleaching procedure and prior to irradiation, I_0 denotes the initial OSL signal measured after X-ray irradiation and stabilization, and $I(t)$ represents the OSL signal measured after a cumulative optical bleaching time t.

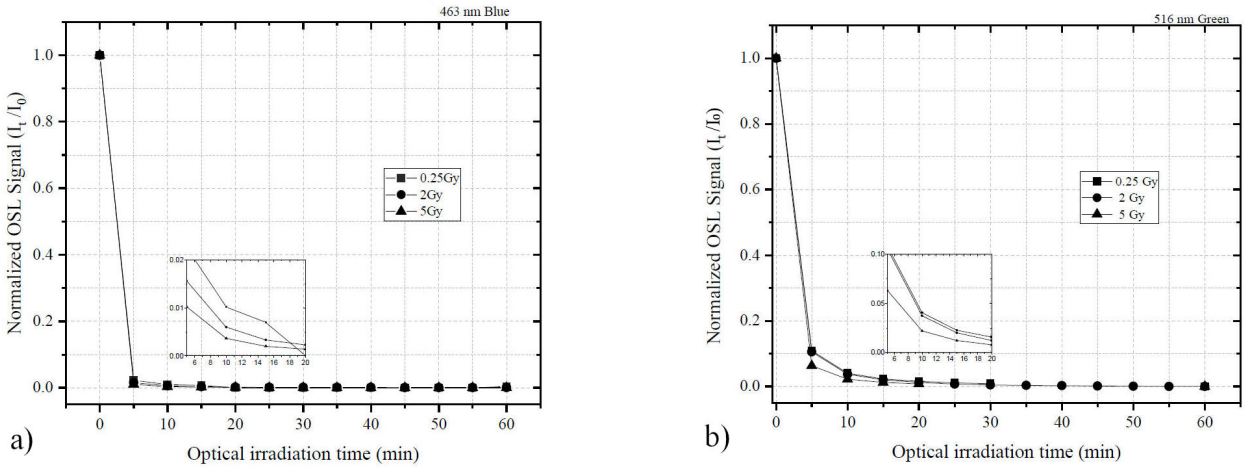


FIGURE 2. Decay of the normalized OSL signal in Al_2O_3:C nanoDot^{TM} dosimeters under optical irradiation at a) 463 nm and b) 516 nm. The curves show the evolution of the remaining signal as a function of cumulative optical irradiation time for the evaluated dose levels.

The initial signal I_0 was defined as the readout obtained immediately after irradiation with 6 MV photons and prior to optical bleaching. The background signal I_b was determined from non-irradiated dosimeters previously conditioned, establishing the baseline level of the measurement system.

To compare the evolution of the bleaching process under different experimental conditions, the ratios $I(t)/I_0$ and $I(t)/I_b$ were calculated. The former represents the fraction of remaining signal relative to the initial signal, while the latter indicates the relationship between the measured signal and the baseline level.

Bleaching efficiency was calculated as:

$$\text{Efficiency}(\%) = \left(1 - \frac{I(t)}{I_0}\right) \times 100.$$

These quantities were used to construct normalized decay curves and comparative tables of residual signal and bleaching efficiency as a function of time and dose.

TABLE I. Normalized residual signal and bleaching efficiency for Al_2O_3:C nanoDot^{TM} dosimeters under optical irradiation at 463 nm. Values are reported as mean ± standard deviation.

Dose (Gy)	Time (min)	$I(t)/I_0$ (mean ± SD)	Efficiency (%)
0.25	5	0.0226 ± 0.0087	97.74
	10	0.0102 ± 0.0013	98.98
	15	0.0070 ± 0.0005	99.30
2	5	0.0156 ± 0.0039	98.44
	10	0.0060 ± 0.0014	99.40
	15	0.0046 ± 0.0008	99.54
5	5	0.0102 ± 0.0015	98.98
	10	0.0036 ± 0.0005	99.64
	15	0.0020 ± 0.0002	99.80

TABLE II. Normalized residual signal and bleaching efficiency for Al_2O_3:C nanoDot^{TM} dosimeters under optical irradiation at 516 nm. Values are reported as mean ± standard deviation.

Dose (Gy)	Time (min)	$I(t)/I_0$ (mean ± SD)	Efficiency (%)
0.25	5	0.1135 ± 0.0188	88.65
	10	0.0457 ± 0.0067	95.43
	15	0.0279 ± 0.0034	97.21
2	5	0.1037 ± 0.0024	89.63
	10	0.0378 ± 0.0003	96.22
	15	0.0234 ± 0.0001	97.66
5	5	0.1212 ± 0.0224	87.88
	10	0.0447 ± 0.0026	95.53
	15	0.0276 ± 0.0033	97.24

3. Results

3.1. Bleaching efficiency

Bleaching efficiency, calculated from the ratio $I(t)/I_0$, shows a clear dependence on the optical irradiation wavelength. The corresponding results are summarized in Tables I and II.

For the 463 nm system, bleaching efficiency exceeds 98% within the first 5 minutes of irradiation, increasing to values between 98.98% and 99.80% at 10–15 minutes, depending on the delivered dose. In contrast, the 516 nm system exhibits lower initial efficiencies, with values ranging from 87.88% to 89.63% at 5 minutes, and from 95.43% to 97.66% at 10–15 minutes.

These results demonstrate that optical irradiation at 463 nm enables a more efficient removal of the OSL signal compared to 516 nm across all evaluated times.

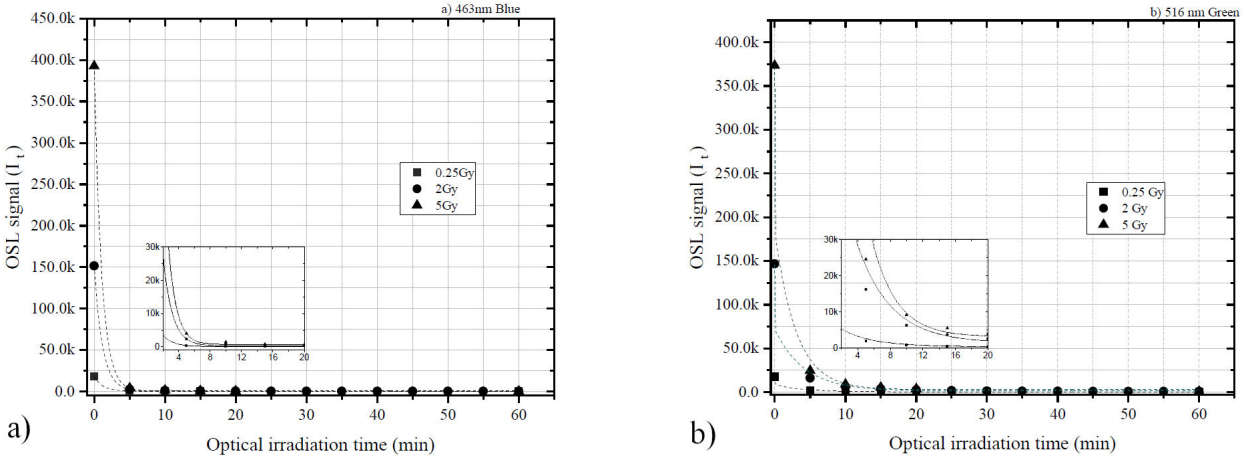


FIGURE 3. Evolution of the OSL signal, $I(t)$, as a function of cumulative optical irradiation time for Al_2O_3:C nanoDot^{TM} dosimeters under optical irradiation at a) 463 nm and b) 516 nm for absorbed doses of 0.25, 2, and 5 Gy. Dashed lines represent monoexponential fits. Insets show the 2–20 min region.

Furthermore, the variation in efficiency with dose is minimal for both wavelengths, indicating that the bleaching process remains consistent within the analyzed dose range.

3.2. Background signal and baseline level

Figure 3 presents the evolution of the OSL signal in absolute units (counts) as a function of optical irradiation time for both wavelengths. A progressive reduction of the signal is observed for all dose levels, with clear differences in decay rate between the two irradiation systems.

The relationship between the residual signal and the system baseline, expressed as $I(t)/I_b$, is summarized in Table III. For the 463 nm system, this ratio decreases rapidly with increasing irradiation time. For a dose of 0.25 Gy, the ratio decreases from 5.86 at 5 minutes to 1.80 at 15 minutes, indicating a close approach to the baseline level. Similarly, for a dose of 5 Gy, values decrease from 57.4 at 5 minutes to 11.1 at 15 minutes.

TABLE III. Residual signal relative to the baseline for Al_2O_3:C nanoDot^{TM} dosimeters. Baseline values were $I_b = 70$ counts at 463 nm and $I_b = 57$ counts at 516 nm.

λ (nm)	Dose (Gy)	Time (min)	$I(t)$ (counts, mean $\pm$ SD)	$I(t)/I_b$
463	0.25	5	410 ± 157	5.86
		10	185 ± 22	2.64
		15	126 ± 8	1.80
	2	5	2364 ± 589	33.8
		10	905 ± 203	12.9
		15	692 ± 116	9.89
	5	5	4012 ± 556	57.4
		10	1423 ± 194	20.3
		15	777 ± 69	11.1
516	0.25	5	1993 ± 330	35.0
		10	802 ± 117	14.1
		15	489 ± 59	8.59
	2	5	16173.93 ± 1597.43	283.9
		10	6241.60 ± 684.23	109.6
		15	3685.93 ± 417.09	64.7
	5	5	24559 ± 3319	431.1
		10	9144 ± 736	160.5
		15	5501 ± 463	96.6

In contrast, the 516 nm system exhibits significantly higher residual-signal ratios throughout the entire time interval. Based on the values of the ratio $I(t)/I_b$ summarized in Table III, the ratio decreases from 35.0 at 5 minutes to 8.59 at 15 minutes for 0.25 Gy, whereas for 5 Gy the corresponding values are 431.1 and 96.6, respectively. These values indicate that, despite the progressive reduction of the OSL signal shown in Fig. 3, the residual signal remains substantially above the baseline level, particularly at higher absorbed doses.

These results indicate that, although both systems reduce the signal over time, irradiation at 463 nm enables a faster approach to the baseline level, whereas at 516 nm a considerably higher residual signal persists across the entire dose range.

This behavior suggests differences in the decay dynamics, which can be further quantified through curve fitting and the determination of characteristic parameters such as the time constant and half-life.

3.3. Monoexponential fitting and half-life

Monoexponential fitting was performed on the normalized decay curves shown in Fig. 2, yielding the parameters τ, $t_{1/2}$, and the residual term, as summarized in Tables IV and V.

For the 463 nm system, the time constant values range approximately from 1.07 to 1.30 min, corresponding to half-life values between 0.74 and 0.90 min. In contrast, for the 516 nm system, the time constants are significantly higher, ranging from 2.14 to 2.35 min, with half-life values between 1.49 and 1.63 min.

This difference indicates that the signal decay process occurs in approximately half the time under 463 nm irradiation compared to 516 nm across the entire evaluated dose range.

The coefficient of determination (R^2) exceeds 0.99 in all cases, indicating an excellent agreement between the monoexponential model and the experimental data.

These results are consistent with the higher bleaching efficiency and faster approach to the baseline level previously observed for the 463 nm irradiation.

TABLE IV. Monoexponential fitting parameters obtained from normalized decay curves under optical irradiation at 516 nm.

Dose (Gy)	τ (min)	$t_{1/2}$ (min)	Residual term	R^2
0.25	2.27 ± 0.12	1.57	0.0101 ± 0.0039	0.9983
0.5	2.35 ± 0.12	1.63	0.0088 ± 0.0037	0.9984
1	2.14 ± 0.08	1.49	0.0119 ± 0.0024	0.9993
2	2.21 ± 0.09	1.53	0.0119 ± 0.0027	0.9991
3	2.15 ± 0.08	1.49	0.0107 ± 0.0025	0.9993
5	2.19 ± 0.25	1.52	0.0092 ± 0.0081	0.9937

TABLE V. Monoexponential fitting parameters obtained from normalized decay curves under optical irradiation at 463 nm.

Dose (Gy)	τ (min)	$t_{1/2}$ (min)	Residual term	R^2
0.25	1.30 ± 0.06	0.90	0.00186 ± 0.00105	0.9999
0.5	1.22 ± 0.05	0.84	0.00211 ± 0.00082	0.9999
1	1.17 ± 0.04	0.81	0.00241 ± 0.00054	0.9999
2	1.17 ± 0.03	0.81	0.00182 ± 0.00046	0.9999
3	1.12 ± 0.03	0.78	0.00145 ± 0.00037	0.9999
5	1.08 ± 0.03	0.75	0.00065 ± 0.00035	0.9999

3.4. Temporal behavior

The shape of the decay curves suggests the presence of multiple trap populations with different emptying probabilities. The rapid initial decrease in signal is associated with shallow traps, while the slower decay region indicates the contribution of deeper or less optically accessible traps.

4. Discussion

The results obtained in this work demonstrate a clear dependence of the optical bleaching process on the irradiation wavelength. Irradiation at 463 nm produced a faster decrease of the OSL signal than irradiation at 516 nm, as shown by the normalized curves $I(t)/I_0$, the bleaching efficiency values, and the kinetic parameters obtained from monoexponential fitting. This behavior indicates that the reduction of the stored signal is strongly influenced by the photon energy of the stimulating light.

From a physical perspective, this wavelength dependence can be associated with the spectral response of optically active traps in Al_2O_3:C. Shorter wavelengths correspond to higher photon energies and therefore increase the probability of optical release of trapped electrons. This interpretation is consistent with the general OSL mechanism described for Al_2O_3:C, where optical stimulation promotes trapped charge carriers into the conduction band or into recombination pathways that produce luminescence [1, 5]. In addition, comparative studies of blue and green stimulation in Al_2O_3:C have reported higher stimulation efficiency in the blue spectral region, supporting the stronger bleaching effect observed at 463 nm [6].

Although the higher bleaching efficiency observed at 463 nm is consistent with the greater photon energy and higher optical stimulation efficiency reported for blue stimulation in Al_2O_3:C, the difference in irradiance between the two optical modules must also be considered. The irradiance at the dosimeter plane was 587.7 mW·cm^{-2} for the 463 nm module and 457.7 mW·cm^{-2} for the 516 nm module, corresponding to an approximately 28% higher irradiance for the 463 nm system. Therefore, the observed differences in bleaching efficiency cannot be attributed exclusively to wavelength effects.

The higher optical power density of the 463 nm module may have contributed partially to the faster signal reduction. Nevertheless, under the experimental conditions evaluated in this work, the 463 nm system produced consistently shorter time constants, lower residual signals, and higher bleaching efficiencies than the 516 nm system. Future studies using power-matched optical irradiation conditions would be necessary to separate the relative contributions of wavelength and irradiance.

The present results demonstrate that optical bleaching significantly reduces the residual OSL signal, facilitating the practical reuse of nanoDot$^{\mathrm{TM}}$ dosimeters within the investigated dose range. However, the long-term lifespan of the detectors was not directly evaluated in this study. The primary objective of this work was to characterize and compare the optical bleaching efficiency of Al_2O_3:C nanoDot$^{\mathrm{TM}}$ dosimeters under 463 nm and 516 nm irradiation, rather than to assess sensitivity degradation or cumulative effects associated with repeated irradiation–bleaching cycles.

Therefore, although the proposed bleaching protocol facilitates dosimeter reuse by reducing the residual signal, conclusions regarding long-term detector lifespan or sensitivity changes cannot be drawn from the present data. Future studies should investigate the effects of repeated irradiation and bleaching cycles on the long-term performance and stability of nanoDot$^{\mathrm{TM}}$ dosimeters.

The kinetic analysis reinforces this interpretation. The time constants obtained for 463 nm irradiation, approximately 1.08–1.30 min, were about half of those obtained for 516 nm irradiation, approximately 2.14–2.35 min. This indicates that the characteristic time scale of trap depopulation is significantly shorter under 463 nm irradiation. Similar wavelength-dependent behavior has been reported for Al_2O_3:C OSL detectors exposed to 6 MV photon beams, where different bleaching wavelengths produced distinct effects on detector response and sensitivity [8].

An important observation is the weak dependence of the normalized decay behavior on dose. The overlap of the normalized curves and the relatively stable values of τ and $t_{1/2}$ across the evaluated dose range suggest that the bleaching kinetics are mainly governed by optically induced transition probabilities rather than by the initial population of trapped charge carriers. This behavior is consistent with continuous-wave OSL descriptions, in which the decay curve reflects the emptying of optically accessible trap populations under a given stimulation condition [1, 4, 5].

The analysis of the ratio $I(t)/I_b$ provides additional insight into the residual signal. For 463 nm irradiation, the rapid decrease of this ratio indicates that the residual signal approaches the baseline level of the reader–dosimeter system within relatively short irradiation times. In contrast, the higher $I(t)/I_b$ values observed for 516 nm, particularly at higher doses, suggest that a fraction of the trapped charge remains in levels that are not efficiently emptied under lower photon energy stimulation.

This behavior can be interpreted in terms of a distribution of trap depths in Al_2O_3:C. Shallow and optically accessible traps are emptied more rapidly and contribute to the initial fast decay of the signal, whereas deeper or less optically accessible traps contribute to the slower residual component.

The presence of multiple trapping and recombination pathways in Al_2O_3:C has been widely discussed in luminescence models and is consistent with the non-zero residual signal observed after prolonged optical irradiation [1, 4, 10, 11].

Additionally, the persistence of residual signal may also be related to phototransfer processes. Such behavior has been reported in Al_2O_3:C under infrared stimulation, where multiple optically stimulated components have been observed, indicating the participation of different trapping states in the luminescence response [7]. The existence of multiple trapping and recombination centers in Al_2O_3:C has been widely discussed in the literature and may contribute to the persistence of residual signal after optical bleaching [1, 10, 11]. However, the specific mechanisms responsible for the residual signal observed in the present study were not directly investigated.

Overall, the results suggest that the observed optical bleaching behavior in Al_2O_3:C nanoDot$^{\mathrm{TM}}$ dosimeters is influenced by the interaction between photon energy, trap-depth distribution, and the photoionization probability of trapped carriers.

The shorter wavelength of 463 nm provides more efficient access to optically active trap populations, leading to faster signal decay, higher bleaching efficiency, and a closer approach to the baseline level. In contrast, irradiation at 516 nm produces slower bleaching and a higher residual signal, suggesting incomplete depopulation of deeper or less optically accessible traps.

5. Conclusions

In this work, the efficiency of the optical bleaching process in Al_2O_3:C nanoDot$^{\mathrm{TM}}$ dosimeters was evaluated using optical irradiation at 463 nm and 516 nm. The results demonstrate that the irradiation wavelength significantly influences both the rate of OSL signal decay and the residual signal level achieved.

Irradiation at 463 nm showed higher bleaching efficiency compared to 516 nm, reaching values above 99% within short irradiation times. This behavior was consistently reflected in the normalized curves, in the efficiency values, and in the $I(t)/I_b$ ratio, where a closer approach to the system baseline level was observed, particularly at low doses.

Kinetic analysis based on monoexponential fitting revealed that the decay process occurs on a significantly shorter time scale for 463 nm, with half-life values approximately two times lower than those obtained for 516 nm. Additionally, the kinetic parameters exhibited low dependence on dose within the evaluated range, suggesting that the bleaching process is primarily governed by optical interaction probability rather than by the initial population of charge carriers.

In contrast, irradiation at 516 nm showed a significant persistence of residual signal, particularly at higher doses, indicating lower efficiency in the emptying of electron traps under these conditions. This effect was evidenced by both the higher values of $I(t)/I_b$ and the longer characteristic times of the process.

Overall, the results confirm that the selection of the optical irradiation wavelength is a determining factor in the optimization of the bleaching process in OSL dosimeters. These findings have direct implications for the design of reuse protocols, enabling a reduction in conditioning times without compromising the stability of the dosimetric response in clinical applications.

1. E.G. Yukihara and S.W.S. McKeever, *Optically Stimulated Luminescence: Fundamentals and Applications* (Wiley, Chichester, 2011).
2. P.A. Jursinic, Characterization of optically stimulated luminescent dosimeters (OSLDs) for clinical dosimetric measurements, *Med. Phys.* **34** (2007) 4594, https://doi.org/10.1118/1.2804555.
3. M.S. Akselrod, V.S. Kortov, D.J. Kravetsky and V.I. Gotlib, Highly sensitive thermoluminescent anion-defective α-Al_2O_3:C single crystal detectors, *Radiat. Prot. Dosim.* **32** (1990) 15.
4. S.W.S. McKeever, *Thermoluminescence of Solids* (Cambridge University Press, Cambridge, 1985).
5. E.G. Yukihara and S.W.S. McKeever, Optically stimulated luminescence (OSL) dosimetry in medicine, *Phys. Med. Biol.* **53** (2008) R351, https://doi.org/10.1088/0031-9155/53/20/R01.
6. N.K. Umisedo, E.G. Yukihara and S.W.S. McKeever, Comparison between blue and green stimulated luminescence of Al_2O_3:C, *Radiat. Meas.* **45** (2010) 181, https://doi.org/10.1016/j.radmeas.2010.02.001.
7. E. Bulur and W. Wahl, Infrared stimulated luminescence from Al_2O_3:C, *Radiat. Meas.* **29** (1998) 639, https://doi.org/10.1016/S1350-4487(98)00059-0.
8. A.A. Omotayo, J.E. Cygler and G.O. Sawakuchi, The effect of different bleaching wavelengths on the sensitivity of Al_2O_3:C optically stimulated luminescence detectors exposed to 6 MV photon beams, *Med. Phys.* **39** (2012) 5457, https://doi.org/10.1118/1.4742865.
9. P.A. Jursinic, Changes in optically stimulated luminescent dosimeter dosimetric characteristics with accumulated dose, *Med. Phys.* **37** (2010) 132, https://doi.org/10.1118/1.3267489.
10. A.J.J. Bos, Theory of thermoluminescence, *Radiat. Meas.* **33** (2001) 737, https://doi.org/10.1016/S1350-4487(01)00106-0.
11. V. Pagonis, G. Kitis and C. Furetta, *Numerical and Practical Exercises in Thermoluminescence* (Springer, New York, 2006).
12. M. Jain, K.J. Thomsen, L. Bøtter-Jensen and A.S. Murray, Thermal transfer and apparent dose distributions in OSL dating of quartz, *Radiat. Meas.* **38** (2004) 101, https://doi.org/10.1016/j.radmeas.2003.10.003.
13. A.A. Mowlavi et al., AAPM Task Group 191: Clinical use of luminescent dosimeters, *Med. Phys.* **47** (2020) e19, https://doi.org/10.1002/mp.13839.
14. International Atomic Energy Agency, *Absorbed Dose Determination in External Beam Radiotherapy: An International Code of Practice for Dosimetry Based on Standards of Absorbed Dose to Water (TRS-398)* (IAEA, Vienna, 2000).